Theoretical and experimental studies of a switched inertance hydraulic system including switching transition dynamics, non-linearity and leakage

Min Pan (min.pan@bath.edu), Nigel Johnston, Andrew Plummer, Sylwester Kudzma, Andrew Hillis

University of Bath

Abstract

This paper reports on theoretical and experimental investigations of a switched inertance device, which is designed to control the flow and pressure of a hydraulic supply. The device basically consists of a switching element, an inductance and a capacitance. It is able to boost the pressure or flow with a corresponding drop in flow or pressure respectively, analogous to a hydraulic transformer. In this paper, an enhanced analytical distributed parameter model in the frequency domain, which includes the effect of switching transition, non-linearity and leakage of the valve, is proposed and validated by simulation and experiments. A flow booster test rig is studied as a typical system. Simulated and experimental results show good performance, and accurate estimation of system pressure and dynamic flowrate can be obtained by using the enhanced analytical model. The model is very effective for understanding, analysing and optimising the characteristics and performance of a switched inertance device. It also can be used to aid in the design of a switched inertance hydraulic system.

Keywords: digital hydraulics; switched inertance hydraulic systems; switching valve; transmission line model; efficient fluid power;

1 Introduction

In most fluid power hydraulic systems, the speed and/or force of a load are controlled using valves to throttle the flow and thus reduce the hydraulic pressure. This is a simple but extremely inefficient method as the excess energy is lost as heat, and it is common for more than 50% of the input power to be wasted in this way [1]. A switched inertance hydraulic system (SIHS), which performs analogously to an electrical 'switched inductance' transformer, is one possible approach to raise efficiency [1-3]. This technique makes use of the inherent reactive behaviour of hydraulic components. A fluid volume can have a capacitive effect, whilst a small diameter line can have an inductive effect [1]. The intention for switching control is to avoid the intrinsic high energy losses which occur if resistance control by metering valves is applied.

Different configurations of SIHS were proposed initially by Brown in 1987 [2]. These devices generally comprised a high-speed switching element, an inductive component and a capacitive fluid volume. Three-port valves and four-port valves were applied as the switching element in the system with one and two inertance tubes respectively. The advantages and disadvantages of the switched hydraulic system have been studied relative to conventional orifice-metered valves. High bandwidth and efficiency are the two main advantages [2]. With a high switching frequency, the switched hydraulic system potentially has a wider bandwidth than the conventional valve controlled system. Unlike conventional valve-controlled systems, an ideal SIHS could have 100% efficiency, but in practice losses due to friction and leakage may be significant.

Two basic modes of SIHS, a flow booster and a pressure booster, have been presented and studied in simulation and experiments [1-5]. These modes can be configured by reversing the inlet and outlet connections in a SIHS. In one mode it acts as a flow booster; in the other it performs as a pressure booster, as shown in Figure 1.

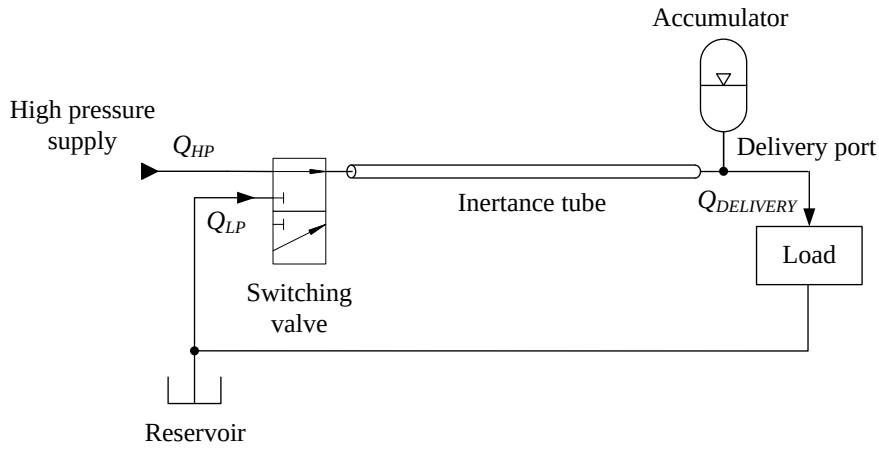

(a) Flow booster

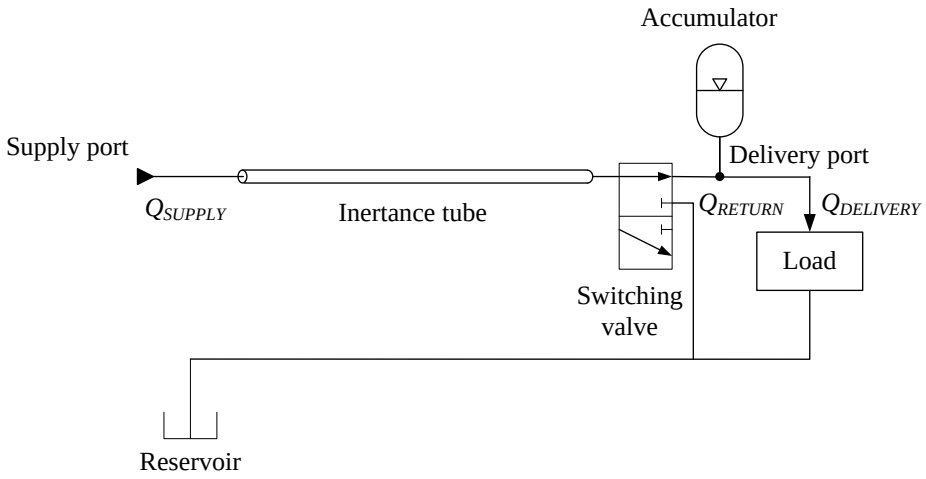

(b) Pressure booster

Figure 1 Schematic diagram of SIHS

Promising results have been achieved with a SIHS in applications [6-8]. However, the dynamics of components have a significant effect on the system performance. A general

study about the components for digital and switching hydraulics can be found in [9]. It showed that the design and performance of the high-speed switching valve is very important for the performance of the SIHS. The valve ideally should have low resistance and low leakage and be able to operate with a very high switching frequency. Numerous valve designs have been proposed for high-speed switching hydraulic systems, including poppet valves, linear spool valves and rotary valves [10-15]. Such high-speed valves give opportunities for improvements in the efficiency of switched inertance hydraulic systems.

Manhartsgruber and Mikota [16] presented a simulation model of a switching control hydraulic system which comprises a switching valve, a long tube and a hydraulic cylinder. A similar modelling method was also applied in Wang et al's work [17]. Comparing the experimental and simulated results, it can be seen that the proposed model is a reliable and accurate method for analysing the detailed dynamic behaviour of a SIHS. However, these models include a set of ODEs describing the actuator dynamics, a 'transmission line method' (TLM) pipeline model and time variant non-linear valve flow equations which may be difficult and time-consuming to solve. Moreover, these models are not easily used to estimate the general characteristics and trends to aid system design. Therefore, an analytical model is desirable for eliminating complex solvers for a set of ODEs, with the aim of being an effective tool for understanding the basic characteristics and design trade-offs for a SIHS. De Negri et al [18] developed an analytical model of a SIHS based on a lumped element model and validated it in experiments based on a pressure booster system. They successfully described the relationship between the flowrate and pressure in a SIHS, but did not focus on system efficiency and power loss.

A mixed time-frequency domain simulation model of a hydraulic buck converter (HBC) was presented in [19]. Time-domain modelling was applied to the switching valve and check valve and frequency-domain modelling was applied to the wave propagation in a pipe. The resulting system of non-linear algebraic equations was solved by using the Newton-Raphson method in combination with a smoothing of the non-smooth properties of the check valve. This method was applied in simulation and can be used for a parametric study of the HBC. Pan et al [20] proposed analytical models of three-port switched inertance hydraulic devices based on a lumped element model and a distributed parameter model in both time domain and frequency domain. The system characteristics, performance and efficiency were studied, investigated and validated by using the analytical models, simulations and experiments. They found that distributed parameter wave propagation effects have a very important and complicated effect on the performance. The results from a test rig showed very promising performance from the SIHS. These models effectively help to understand the physical characteristics of SIHS and introduce a useful tool to analyse the effect of system parameters. However, the effects of switching transition, non-linearity and leakage in the valve, which could affect system dynamics and result in more energy loss, were not considered in the previous analytical models.

This paper develops an analytical model of a three-port switched inertance hydraulic device with the consideration of switching transition, non-linearity and valve leakage effects. Firstly a frequency-domain distributed parameter model is introduced for investigating ideal instantaneous switching operation, and the problems and limitations are presented and discussed. This is described as the ‘basic analytical model’. This is

followed by an improved analytical model with the effect of switching dynamics and non-linearity and leakage of the valve. This is described as the 'enhanced analytical model'. The system pressure, dynamic flowrate, flow loss and power loss are predicted by using the enhanced analytical model and compared to simulations. Experimental validation is presented and followed by discussion and conclusions.

2. Basic analytical model

An analytical model of an ideal SIHS was proposed in [20]. The model is based on frequency-domain analysis and transformation to the time domain. The following assumptions are made.

- The high and low pressure supply ports of the switching valve have the same resistance R_v;
- The resistance R_v is linear and time-invariant;
- Switching occurs instantaneously;
- The supply pressures p_H, $p_L$and the delivery pressure p_d are constant;
- There is no valve leakage across the ports.

Figure 2 shows a schematic of an analytical SIHS model where the system resistances of the high-speed switching valve and tube are represented by R_v and R_t, and I represents the tube inertance.

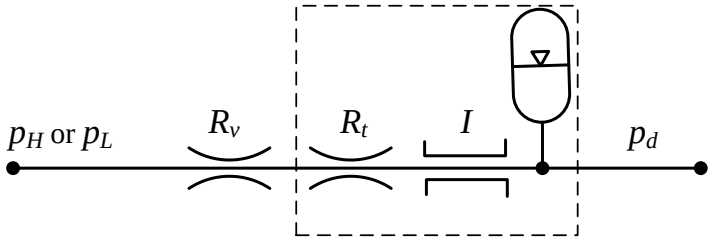

Figure 2 Schematic of an analytical SIHS model

The theoretical supply pressure is shown in Figure 3, where the switching transition and leakage are not considered [18, 20]. Taking the Fourier series of the supply pressure *p*, the Fourier coefficient P_n is:

$$P_n = \frac{p_H}{2\pi nj}(1-e^{-j2\pi n\alpha}) + \frac{p_L}{2\pi nj}(e^{-jn2\pi\alpha} - e^{-jn2\pi}) \tag{1}$$

where α is the switching ratio of SIHS.

The Fourier coefficient Q_n of the flowrate can be described by using Equation (2)

$$Q_n = \frac{P_n}{Z_E} \tag{2}$$

where Z_E is the entry impedance which is the ratio of the pressure ripple to the flow ripple at the entry to the hydraulic circuit [21].

For a distributed parameter model, the entry impedance Z_E is given by Equation (3):

$$Z_E = jZ_0\xi\tan(\frac{\omega L\xi}{c}) + R_v \tag{3}$$

where $Z_0 = \frac{\rho c}{A}$ is the pipe characteristic impedance and ξ is the viscous wave correction factor [22].

$$\xi = \left(1 - \frac{2}{z}\frac{J_1(z)}{J_0(z)}\right)^{-\frac{1}{2}} \text{ and } z = jr\sqrt{\frac{j\omega}{\nu}} \tag{4}$$

Substituting Equation (1) and (3) into Equation (2), the Fourier coefficient Q_n is given in Equation (5).

$$Q_n = \frac{p_H(1-e^{-j2\pi n\alpha}) + p_L(e^{-jn2\pi\alpha} - e^{-jn2\pi})}{2\pi nj(jZ_0\xi\tan(\frac{\omega L\xi}{c}) + R_v)} \tag{5}$$

The flowrate $q(t)$ in the time domain at the connection between the valve and the inertance tube can be obtained by using Fourier series:

$$q(t) = 2\sum_{n=1}^{\infty} Q_n e^{\frac{jn2\pi \cdot t}{T}} + q_m \tag{6}$$

where q_m is the mean delivery flowrate and T is the switching cycle period. An example of the predicted flowrate based on equations (1)-(6) is shown in figure 3. Pulsations due to wave transmission effects can be seen clearly; the precise shape of the flowrate waveform will depend on several factors including the tube length and switching frequency.

For comparison with this analytical model, a time domain numerical simulation model was created using MATLAB Simulink [20]. The high-speed switching valve was assumed to switch instantaneously and the switching valve flow was modelled using the equation (7).

$$q_V(t) = \frac{\Delta p}{R_v} \tag{7}$$

where Δp is the pressure difference through the valve.

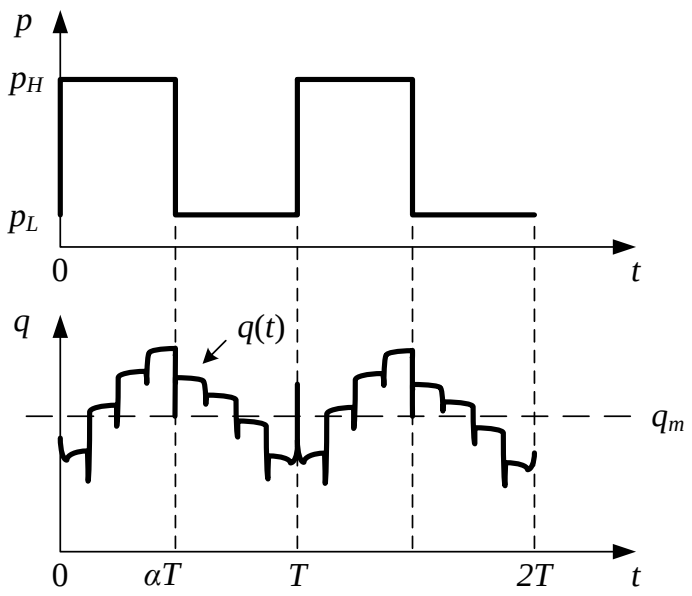

Figure 3 Supply pressure and example of flow rate with an ideal instantaneous switching transition

The Transmission Line Method (TLM) was used to model the wave propagation in the tube. The model was developed by Krus et al [23] and modified by Johnston [24] to include unsteady or frequency-dependent friction. This model accurately and efficiently represents wave propagation and laminar friction over a very wide frequency range. However, the previous TLM models have some inherent inaccuracies [23, 24]. An improved alternative TLM model has been proposed by Johnston [25], and it was used to model the inertance tube in the following simulation work. A small compressible volume ($5cm^3$) was included between the valve model and the TLM inertance tube model and a large volume ($0.02\ m^3$) was included at the load. The high supply pressure p_H was fixed at 100bar, the low supply pressure p_L at 50bar and the average delivery flow was set at 20L/min in the simulation. The constant linear resistance of the valve was assumed as 20 bar/(L/s). Based on Nyquist's theorem and the timestep used in the

time-domain simulation, 400 spectral components were sufficient and were used in the frequency domain model. The parameters in Table 1 were used for the simulated and analytical models. Figure 4 shows the results obtained by using the analytical model and simulation in one switching. The mean flowrates from the high pressure and low pressure supplies are also shown.

Table 1 Parameters for analytical SIHS model

Density ρ	870 kg/m^3
Viscosity v	32 cSt
Switching frequency f	100 Hz
Speed of sound c	1350 m/s
Switching ratio α	0.5
Inertance tube length L	1 m
Inertance tube diameter d	10 mm
Switching valve orifice area A	0.337 cm^2
Sample frequency	20 kHz
Number of spectral components	400

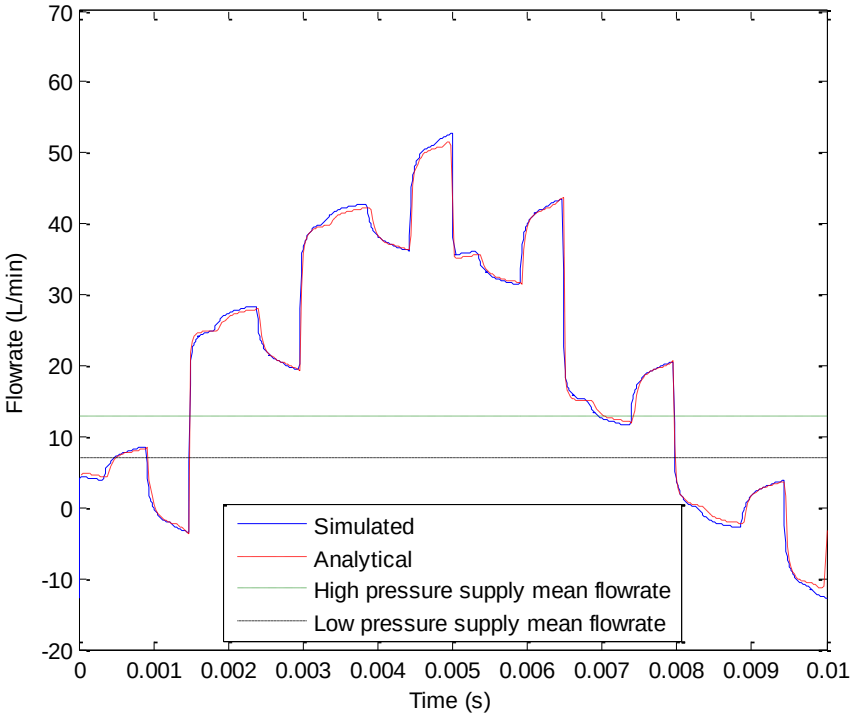

Figure 4 Comparison of dynamic flowrate using analytical and simulated models

As can be seen, the analytical and simulated results agree well. The effect of wave propagation can be seen clearly in figure 4. The analytical model is effective for estimating the dynamic flowrate, and also can be applied for predicting other system characteristics and efficiency. However, the dynamics of valve closure and opening during the switching transition are not considered in this model. Furthermore, the leakage and non-linearity of the valve are also not included. These may significantly affect system efficiency and power consumption in real applications. Enhanced models are proposed in the following section which includes the switching dynamics, leakage and non-linearity of the valve.

3. Enhanced model

In practice the opening and hence the resistance of the valve will vary with time as the ports open and shut, and the opening of the two supply ports may be different. Cross-

port leakage is likely to occur and the leakage resistance will vary with time. Also the valve pressure-flow characteristic for a given opening will be non-linear. These time-dependent properties and non-linear characteristics cannot be modelled directly in the frequency domain. Instead, a mixed time domain and frequency domain approach is proposed, in which the linear parts are modelled in the frequency domain, the non-linear and time dependent parts are modelled in the time domain, and an iterative technique is used to link them.

3.1 Valve opening area

A simple approximation to the cyclic variation in the valve opening areas is shown in Figure 5. Each of the two ports connects to a constant pressure supply, at a high pressure and low pressure respectively, through a time-varying area as shown in figure 5(a). There may be some 'underlap' resulting in a cross-coupling between the ports during the transition, and there may be a small leakage path when the port is nominally closed. It is beneficial for efficiency and stability if as much of the modelling as possible can be done in the frequency domain rather than the time domain. In the analytical model a transformation is made so that there is a 'main' flow path and a 'leakage' flow path. The supplies at the 'main' and 'leakage' path are switched in an opposing manner between high and low pressure, and these switched supplies can be represented readily in the frequency domain. This transformation is made so that the time-dependent variations in the valve openings are less significant, as shown in figure 5(b), resulting in a far more stable and efficient solution. Parameters for the simulation and analytical models are listed in Table 2.

Table 2 Parameters for simulation and analytical models

Density ρ	870 kg/m^3
Viscosity v	32 cSt
Switching frequency f	100 Hz
Speed of sound c	1350 m/s
Switching ratio α	0.5
Inertance tube length L	1 m
Inertance tube diameter d	10 mm
High supply pressure	100 bar
Low supply pressure	50 bar
Delivery flowrate	20 L/min
Switching valve orifice area A	0.337 cm^2
Switching valve leakage area A_{leak}	0.013 cm^2
Valve switching transition time t_{tr}	0.35 ms
Sample frequency	20 kHz
Number of spectral components	400

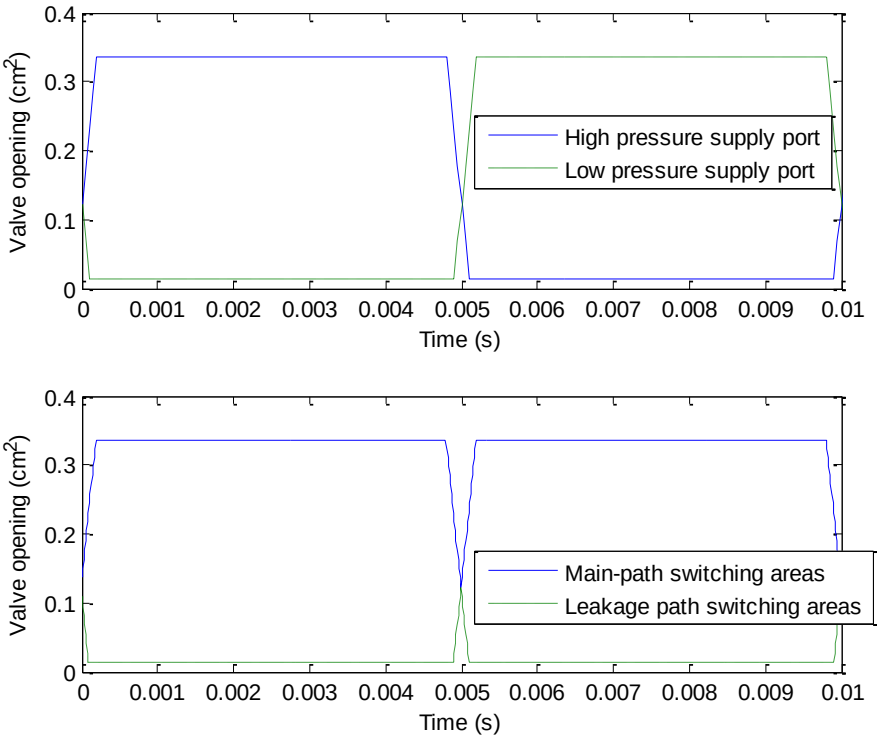

Figure 5 Valve opening during one switching cycle, with slight underlap and cross-port leakage

This can be modelled as shown in Figure 6 (a). Two pressure sources p_1 and p_2, as given by equation (8), were applied in the analytical model. p_1 represents the 'open' port and p_2 represents the 'closed' port with leakage from that port to the outlet port.

$$p_1 = \begin{cases} p_H & 0 \le t \le \alpha T \\ p_L & \alpha T < t \le T \end{cases}$$

$$p_2 = \begin{cases} p_L & 0 \le t \le \alpha T \\ p_H & \alpha T < t \le T \end{cases} \tag{8}$$

In Figure 6 (a), q_i and p_1' are the inlet flowrate and pressure of the inertance tube. The varying resistances R_{tr} and R_u represent the switching transition and underlap between the ports of the main path and the leakage path, and R_{non1} and R_{non2} represent the non-linear characteristics of the valve. Here the linear time invariant part is shown within the

dotted line, and the non-linear time variant part is shown within the dashed lines. The linear time invariant part can be represented as a transfer function in the frequency domain. Using the Fourier transform P_1' of the inlet pressure p_1', the flowrates q_i , q_2 and q_1 can be determined. Figure 6 (b) shows the block diagram which was solved iteratively. For the first iteration, $p_1' = p_1$ and $P_1' = P_1$.

$$q_i = \mathrm{IFFT}\left(\frac{P_1^{'}}{Z_E}\right) \tag{9}$$

$$q_2 = C_d A_{leak}\sqrt{\frac{2\left|p_2 - p_1^{'}\right|}{\rho}}\,\mathrm{sgn}(p_2 - p_1^{'}) \tag{10}$$

$$q_1 = q_i - q_2 \tag{11}$$

However the pressures p_1' and p_2' depend on the non-linear time variant parts.

$$p_{1(k+1)}^{'} = \lambda\left(p_1 - \frac{\rho q_{1(k)}\left|q_{1(k)}\right|}{2C_d^2 A^2}\right) + p_{1(k)}^{'}(1-\lambda) \tag{12}$$

$$p_{2(k+1)}^{'} = p_2 - p_{1(k+1)}^{'} \tag{13}$$

where k is the index of iteration and λ is a relaxation factor for stability. In the following investigations, λ is equal to 0.05.

The entry impedance Z_E is given by equation (14).

$$Z_E = jZ_0\xi\tan(\frac{\omega L\xi}{c}) \tag{14}$$

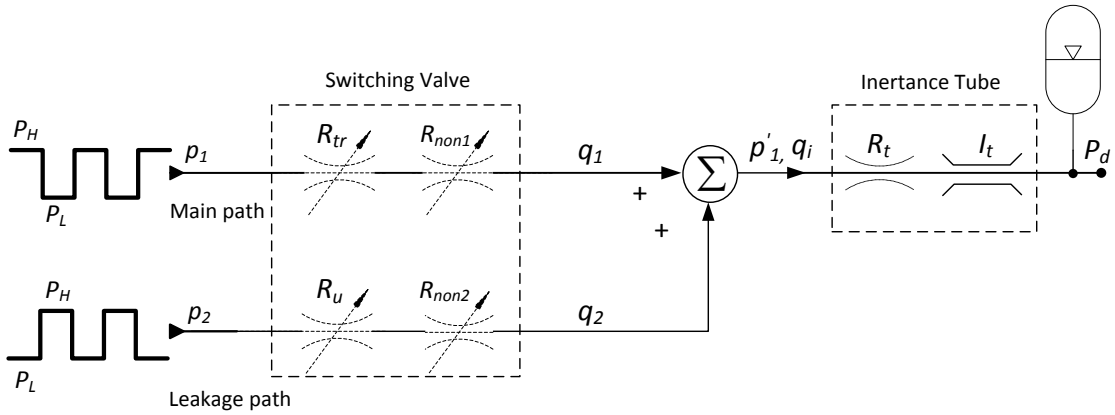

(a) Enhanced analytical SIHS model

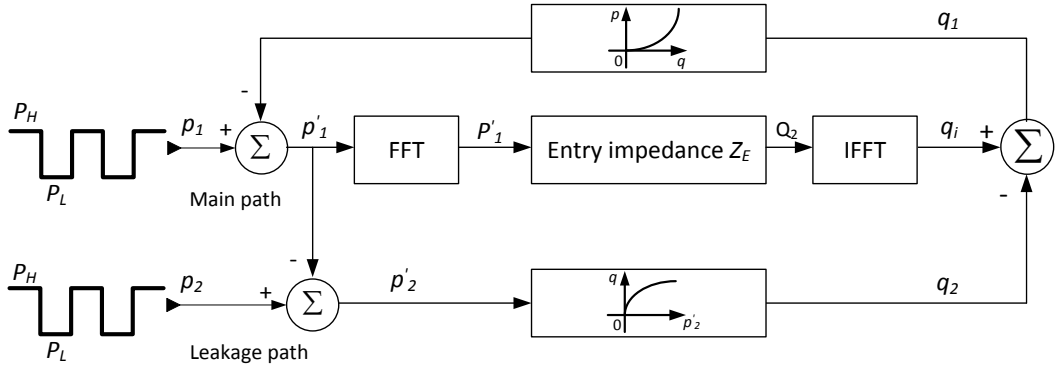

(b) Block diagram representing iterative technique

Figure 6 Schematic of enhanced analytical SIHS model

3.2 Flow volumes

In simulation, a small compressible volume was included between the valve model and the TLM inertance tube model and a large volume was included at the downstream load to maintain a constant delivery pressure. This may result in a difference between the simulated and analytical results [20]. In this section, the volume effect is considered in the analytical model.

For a distributed parameter model, the inertance tube can be represented by a two-port model. The four variables P_i ,Q_i, P_d and Q_d are the complex harmonic amplitudes of

the pressure and flowrate at the inlet and outlet ports. The transmission matrix **T** is defined by the following equation:

$$\begin{pmatrix} P_i \\ Q_i \end{pmatrix} = \begin{pmatrix} \cos\dfrac{\omega L\xi}{c} & jZ_0 \sin\dfrac{\omega L\xi}{c} \\ \dfrac{j}{Z_0}\sin\dfrac{\omega L\xi}{c} & \cos\dfrac{\omega L\xi}{c} \end{pmatrix} \begin{pmatrix} P_d \\ Q_d \end{pmatrix} \tag{15}$$

The relationship of the entry impedance Z_E' and the end impedance Z_{END} can be obtained by using equation (16).

$$Z_E^{'} = \frac{Z_{END}\cos\dfrac{\omega L\xi}{c} + jZ_0 \sin\dfrac{\omega L\xi}{c}}{\dfrac{jZ_{END}}{Z_0}\sin\dfrac{\omega L\xi}{c} + \cos\dfrac{\omega L\xi}{c}} \tag{16}$$

The end impedance can be represented as:

$$Z_{END} = \frac{B}{j\omega V_{end}} \tag{17}$$

where V_{end} is the end volume of the tube. This assumes that the load impedance is very high compared with the volume impedance and so has a negligible effect.

Substituting equation (17) into equation (16), the entry impedance of the system shown in figure 6 can be given by equation (18).

$$Z_E^{'} = \frac{\left(Z_0\omega V_{end}\sin\dfrac{\omega L\xi}{c} - B\cos\dfrac{\omega L\xi}{c}\right)j}{B\sin\dfrac{\omega L\xi}{c} + Z_0 V_{end}\omega\cos\dfrac{\omega L\xi}{c}} \tag{18}$$

The effect of the small upstream volume between the valve and tube can be also included by adding the volume impedance in parallel with the entry impedance (equation (18)). Therefore, the entry impedance of the inertance tube including the upstream and downstream volumes can be calculated as:

$$Z_E = \frac{BZ_E^{'}}{B + jZ_E^{'}\omega V_{up}} \tag{19}$$

where V_{up} is the volume upstream of the tube.

Substituting equation (19) into equation (2), the effect of flow volumes is included in the enhanced analytical model.

The time domain numerical simulation model was modified to include the valve non-linear characteristics, switching transition dynamics and time-dependent leakage. A small compressible volume (5cm^3) was included between the valve model and the TLM inertance tube model and a large volume (0.02 m^3) was included at the load (this can be considered to be equivalent to a small gas-filled accumulator). Parameters for the simulation and analytical model are listed in Table 2 and the valve area shown in Figure 5 was used. It was found that the high frequency spectral components can result in system instability in the iterations if the small compressible volume is included upstream of the inertance tube, because the entry impedance Z_E becomes small at high frequency. Two zero-phase digital filters were used for reducing the effect from the high spectral components for the main path and leakage path.

Figure 7 shows the simulated and analytical inlet flowrate of the inertance tube. A very good agreement was obtained between the simulated and analytical results, which show that the non-instantaneous switching transition dynamics, the non-linearity and leakage of the switching valve are predicted well using the enhanced analytical model. The slight differences are mainly caused by the truncation of the Fourier series in the analytical model and small inaccuracies in the TLM model. It can be concluded that the

enhanced analytical model should be effective for predicting, investigating and optimising the characteristics and performance of a SIHS. A comparison of the inlet flowrate by using the basic and enhanced model is also shown in figure 7. As can be seen, with the modelled high-speed and low resistance switching valve, the flow booster is able to perform and boost the delivery flowrate effectively. However, the valve leakage results in some energy loss and affects the supply flowrate from the high and low supply pressure ports. This can be also found with a comparison of the mean supply flowrates in figure 4 and 7.

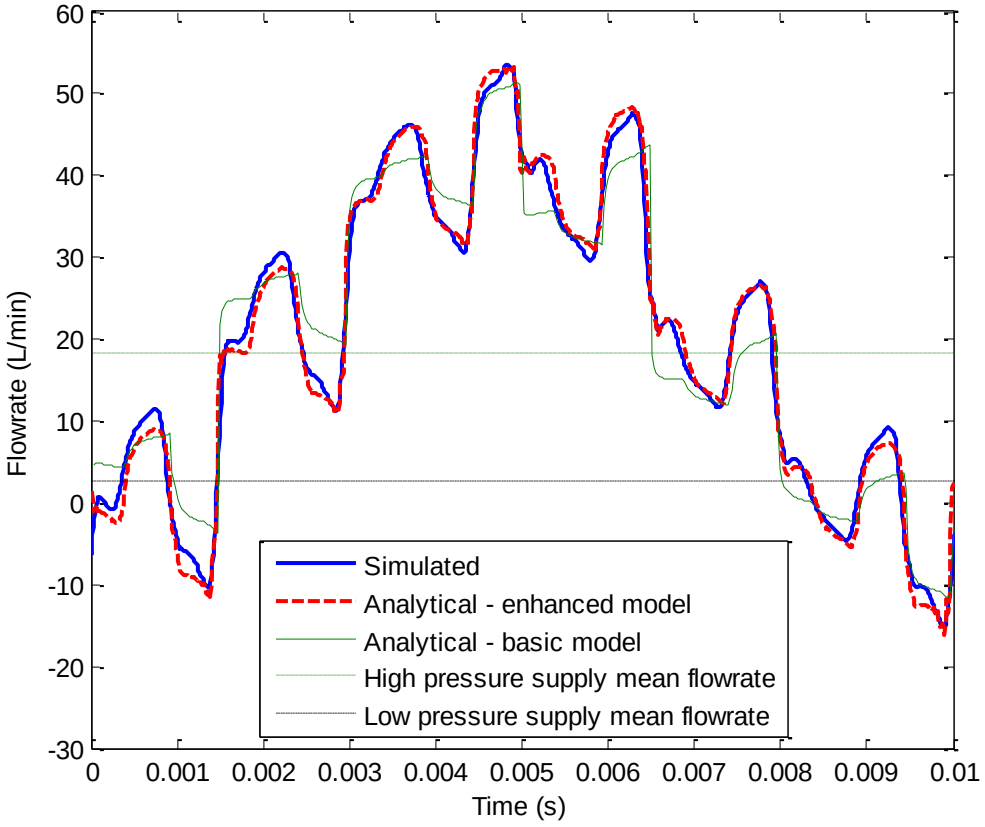

Figure 7 Simulated and analytical inlet flowrate of the inertance tube. Mean supply flowrates for the enhanced analytical model are also shown.

The analytical inlet flowrates of the inertance tube for a range of different delivery flowrates using the enhanced model are shown in figure 8. The shape of the curves

varies significantly at different working conditions. This is affected by the switching transition dynamics of the high-speed valve. For the 'basic' model with instantaneous switching, the shape of the curves would be unaffected by the flowrate.

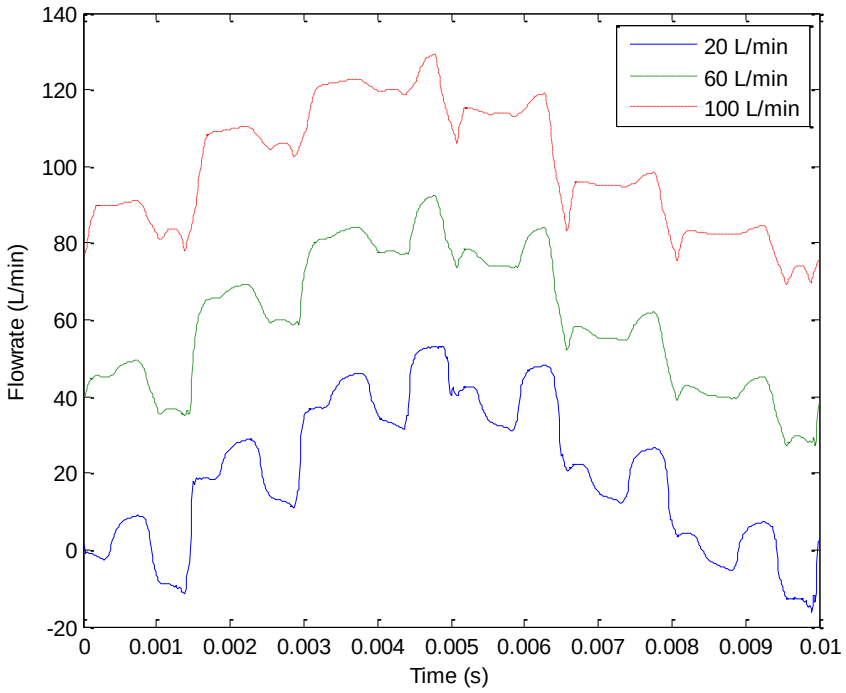

Figure 8 Analytical inlet flow rates of the inertance tube with different delivery flowrates using the enhanced model

4 System performance and optimisation

The performance and optimisation of a SIHS was investigated by using the enhanced analytical model. The parameters in Table 2 were re-applied for the simulated and analytical models. The system flow loss, efficiency and power loss were investigated. As the previous research stated [17, 20], the system flow loss can be defined as:

$$q_{loss} = \bar{q}_H - q_m \alpha \tag{20}$$

or

$$q_{loss} = q_m (1-\alpha) - \bar{q}_L \tag{21}$$

which represents the extra flow rate supplied from the high pressure port relative to the ideal flowrate.

The switching transition dynamics were assumed to be the same with different switching ratios. Using the enhanced analytical model, the system flow loss is shown in Figure 9, where the switching frequency is fixed at 100Hz and the switching ratio varied from 0 to 1 with the step of 0.01. The result obtained from the basic analytical model is also plotted for comparison. For the basic model, the flow loss is independent of the delivery flow rate [20], and the curve is symmetrical with the highest flow loss at a switching ratio of 0.5. As can be seen, the flow loss is greater for the enhanced model, and increases with delivery flowrate. The highest flow loss occurs with the switching ratio of 0.52 – 0.53 and the curve is asymmetric. This shows that the flow loss is increased because of the switching transition, non-linearity and leakage of the valve. More system flow loss is expected when the valve performs with a slow switching speed, high resistance and a low bandwidth.

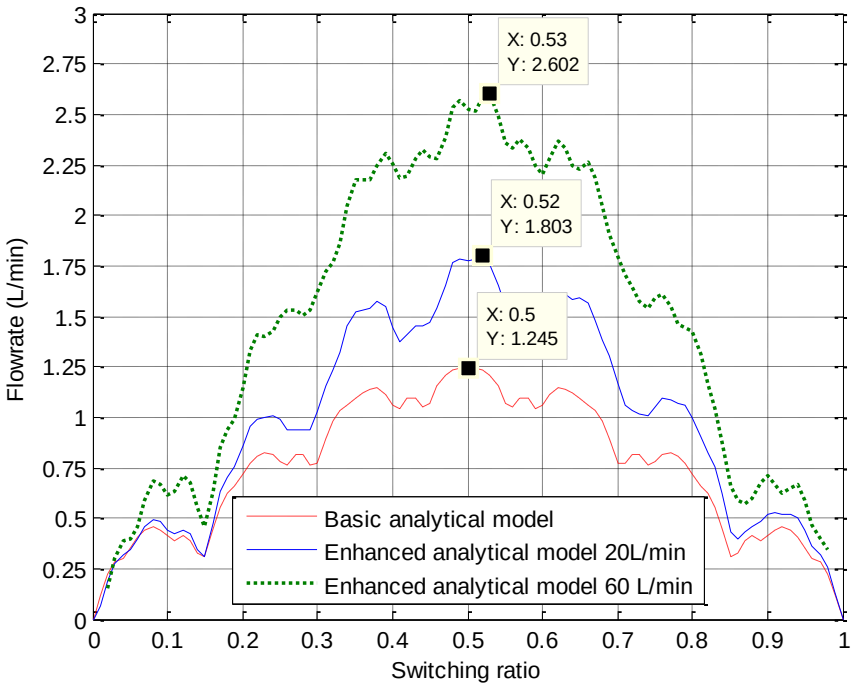

Figure 9 Comparison of flow loss by using the basic and enhanced analytical models with different delivery flowrates

Consider system power loss:

$$W_{loss} = p_H q_H + p_L q_L - p_d q_d \tag{22}$$

or [20]

$$W_{loss} = (p_H - p_L) q_{loss} + q_m^2 R_{overall} \tag{23}$$

where $R_{overall} = \int_0^T R(t)dt$ is the estimated overall system resistance of the main path.

Figure 10 shows the relationship of switching ratio, switching frequency and power loss. Unlike the symmetrical characteristics of flow loss (or power loss) in an ideal instantaneous switching system [17, 20], the power loss is asymmetrical.

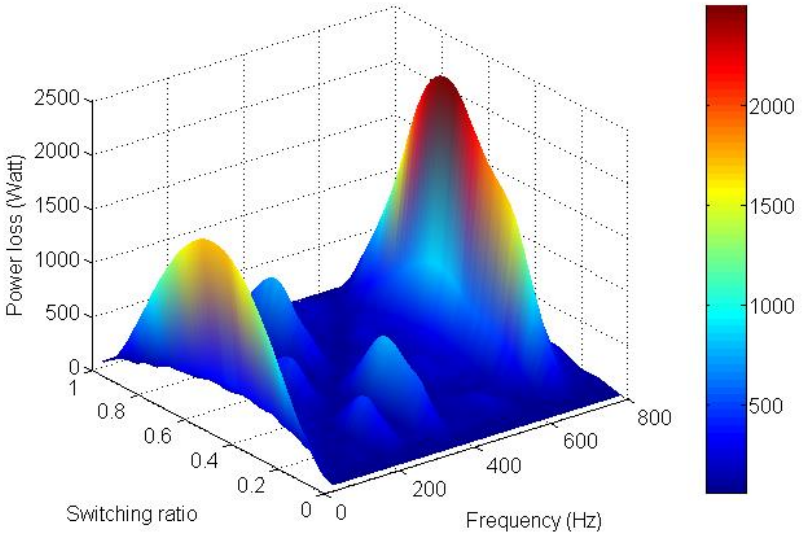

Figure 10 Analytical results of power loss with varying switching frequency and ratio with a delivery flowrate of 20L/min

The ideal optimal switching frequencies for the basic model are given by the following equations [17, 20]:

$$f = \begin{cases} \dfrac{\alpha c}{2L} & 0 \le \alpha \le 0.5 \\ \dfrac{(1-\alpha)c}{2L} & 0.5 < \alpha \le 1 \end{cases} \tag{24}$$

where c is the speed of sound, L is the length of the inertance tube and α is the switching ratio. Optimal switching frequencies for the enhanced model were estimated from the data used to generate figure 10. Table 3 shows the optimal switching frequencies from equation (24) and the optimal switching frequencies for the enhanced model, for different switching ratios. The difference between the optimal switching frequencies for the two models is very small.

Table 3 Optimal switching frequencies with different switching ratios

(Inertance tube length L=1 m; speed of sound c=1350 m/s)

Switching ratio	0.1	0.2	0.3	0.4	0.5	0.6	0.7	0.8	0.9
Ideal switching frequency from the basic model (Hz)	67.5	135	202.5	270	337.5	270	202.5	135	67.5
Switching frequency from the enhanced model (Hz)	68.5	136	202.5	269.5	338.5	270.5	203.5	136	68.5

Figure 11 shows the comparison of flow loss using the enhanced model with a fixed switching frequency of 100Hz, the varying optimal switching frequencies for the enhanced model and the ideal optimal switching frequencies for the basic model. The delivery flowrate was fixed at 20L/min. As can be seen, the flow loss with the ideal optimal switching frequencies is much lower than using a fixed switching frequency of 100Hz. Slightly more efficient results can be achieved when the optimal switching frequencies are estimated using the enhanced model, but the difference is small and it may be acceptable to use the much simpler equation which was derived for the basic model, equation (24).

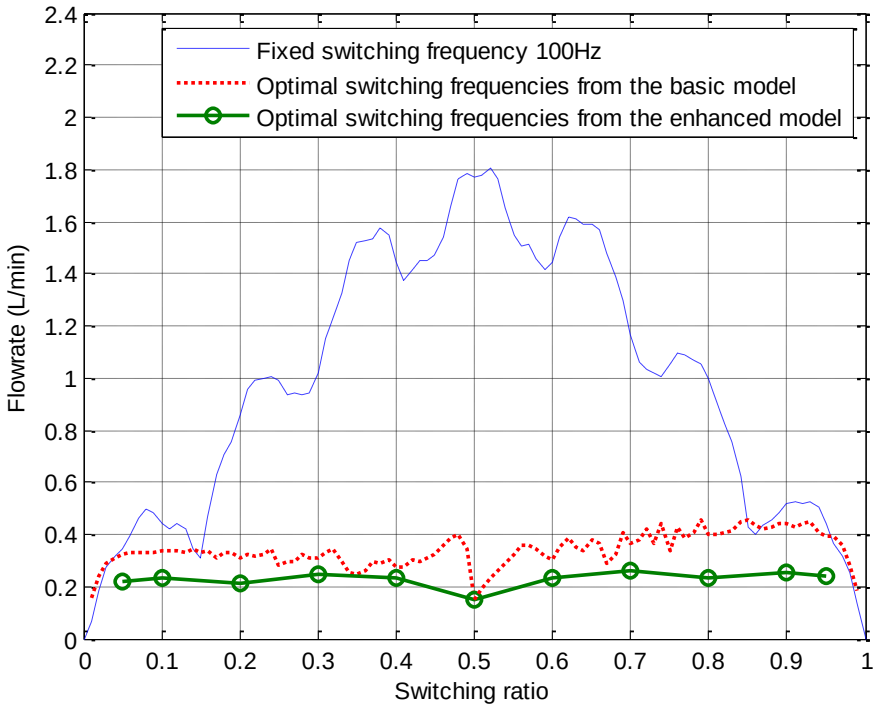

Figure 11 Comparison of flow loss for the enhanced model using a fixed switching frequency (100Hz), optimal switching frequencies from the basic model and optimal switching frequencies from the enhanced model

Analytical characteristics of the SIHS using the basic and enhanced analytical model are shown in Figure 12 for different switching ratios (0.3, 0.5 and 0.9) and a fixed switching frequency of 337.5 Hz. The lines represent the results from the basic analytical model and the triangle and circle symbols represent the results from the enhanced analytical model with a constant delivery flowrate of 0.5L/s and 1L/s, respectively. As can be seen, lower system efficiency and higher system power loss occurred when the switching transition dynamics, non-linearity and leakage of the valve were included. More system power loss occurred when a higher loading flowrate was applied. However, the SIHS maintained high efficiency (over 80%) with a large range of delivery flowrate with an optimal switching frequency of 338 Hz and a ratio of 0.5. It can be concluded that a

well-designed SIHS is very effective and energy efficient. The enhanced analytical model can be used to aid in the design of a SIHS.

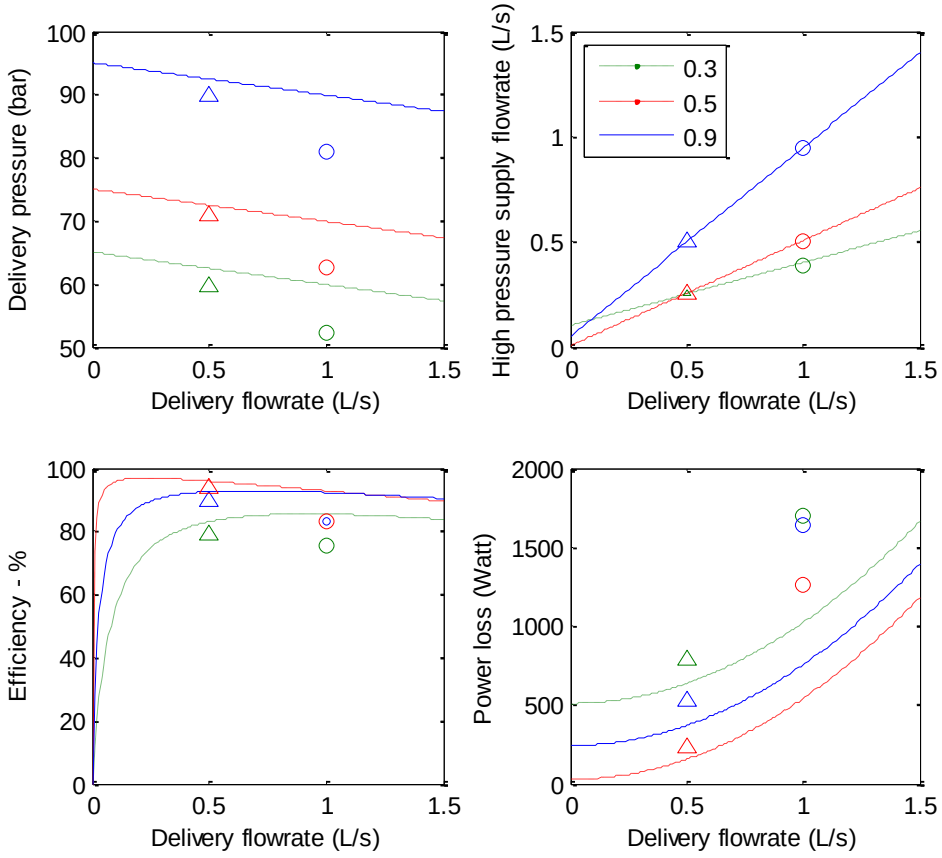

Figure 12 Analytical results of a SIHS based on the basic and improved analytical model, 337.5 Hz switching frequency (lines: basic model; symbols: enhanced model)

5 Experimental validation

5.1 Switching valve

The proportional directional valve series DF*plus* D1FP from Parker Hannifin was used as a switching valve. Figure 13 shows the characteristics of the valve when the valve is fully open to the port A and B. Similar resistances of the high and low pressure supply ports of the switching valve can be assumed.

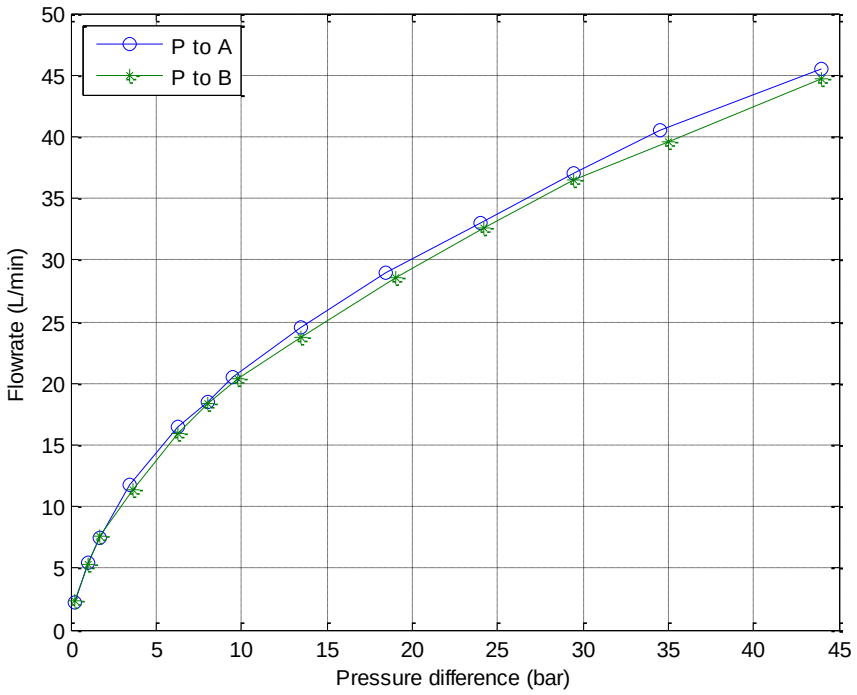

Figure 13 Valve characteristics with a 100% opening

To ensure a short switching time, only 20% opening was demanded. However, a large valve resistance is expected with only 20% opening. Figure 14 shows the measured valve spool responses to a 20Hz square wave demand with a switching ratio of 0.5. The transition switching period is shown clearly and the switching rise time is about 2ms.

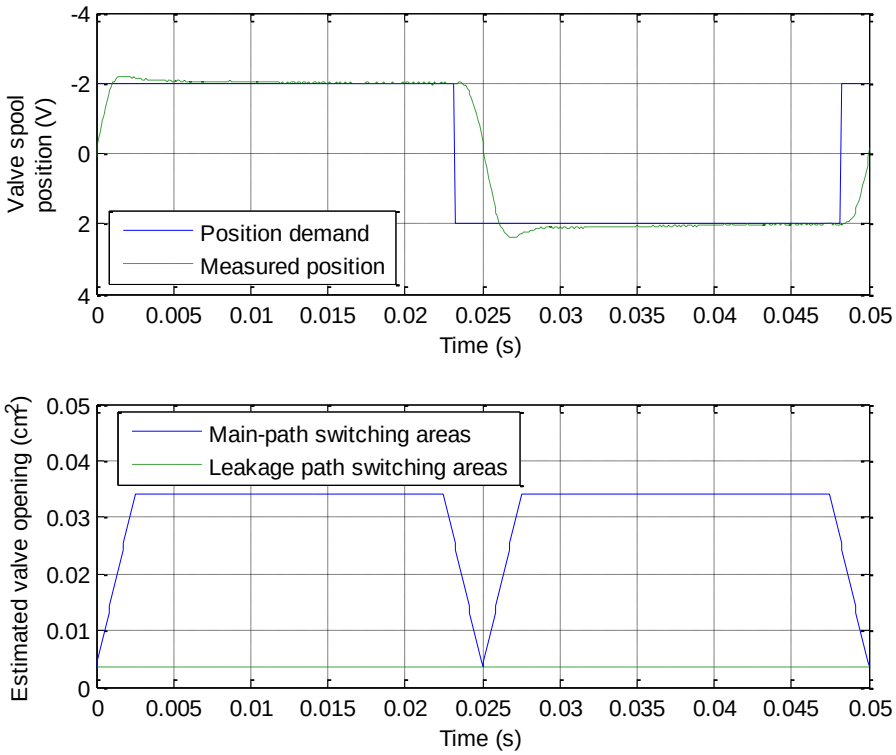

Figure 14 Valve spool position and approximated valve opening areas with a switching ratio of 0.5 and a switching frequency of 20Hz

Figure 14 also shows the approximated valve opening areas. A zero lap is assumed between the opening of the high and low pressure supply ports and both ports have non-linear pressure/flow characteristics.

A flow booster configuration was constructed as the test rig, as shown in Figure 15. The system mainly comprised the proportional valve, an inertance tube comprising two rigid tubes connected in series, and a loading system comprising a pressure compensated flow control valve and a needle valve. Experiments were carried out to verify the analytical model. Figure 16 shows a photograph of the experimental rig.

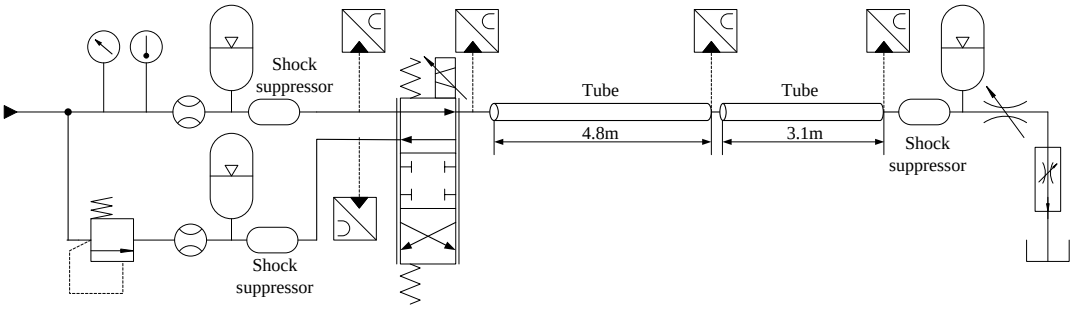

Figure 15 Schematic of the test rig in flow booster configuration

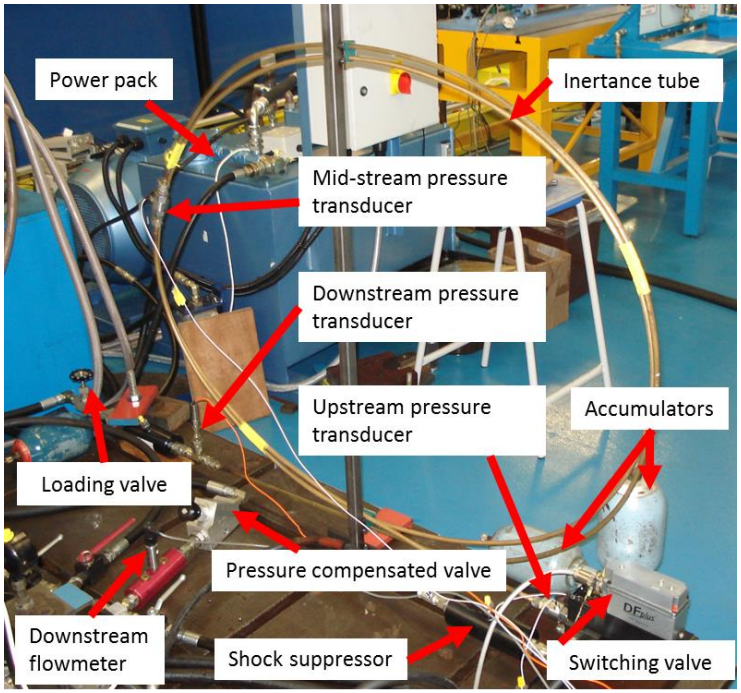

Figure 16 Photograph of the experimental rig

A hydraulic power pack with a maximum supply pressure of 300 bar was used as the high pressure supply source, and the low supply pressure was controlled by the pressure reducing valve. Three accumulators and in-line shock suppressors were used to maintain constant pressures at the high pressure supply, low pressure supply and load. The initial charging pressures of the accumulators were 60 bar, 20 bar and 35 bar respectively, and half the charging pressures of the accumulators, i.e. 30 bar, 10 bar and 17.5 bar, were applied to the shock suppressors.

The inertance tube consisted of two pipe sections with lengths of 4.8m and 3.1m, with a pressure transducer between them, arranged in a large loop of approximately 1m diameter. This is significantly longer than would be used in a practical application, because the switching valve used has a slower response than desired. In more realistic applications, the switching frequency might be over 100Hz and the inertance tube length of the order of 1 m, but this would require a higher performance valve. However the valve used here was sufficient for proof of principle.

Three miniature piezoresistive pressure transducers (Measurement Specialties *EPX*series EPX-N03) with a calibrated pressure range of 100 bar, were used to measure the supply, upstream pressure between the switching valve and the tube and the mid-stream pressure at the connection. Another sensor with a pressure range of 35 bar was used to measure the low supply pressure. The downstream pressure was measured by a Druck high performance *PDCR* series transducer with a calibrated pressure range of 100 bar. Two gear flow meters were applied for the measurement of upstream flowrates. The one connected to the low supply pressure port has a flowrate range from 0.1L/min to 7L/min, whilst the one connected to the high supply pressure port has a range of 0.5 L/min to 70 L/min. Parameters for the analytical model and experiments are listed in Table 4.

Table 4 Parameters for the analytical model and experiments

Density ρ	860 kg/m^3
Viscosity v	38 cSt
Switching frequency f	20 Hz
Inertance tube length L	7.9 m
Inertance tube diameter d	7 mm
Speed of sound c	1300 m/s
Oil temperature	40 °C

5.3 Experimental results

The high supply pressure was fixed at 62 bar and the low pressure at 23 bar. Firstly the needle valve was fully closed to ensure no flowrate through the system. The switching frequency was fixed at 20Hz and the switching ratio of 0.5 was applied.

Figure 17 shows the experimental upstream inlet pressure of the inertance tube with a comparison of analytical results from the basic and enhanced analytical models. Parameters for the basic analytical model can be found in [20].

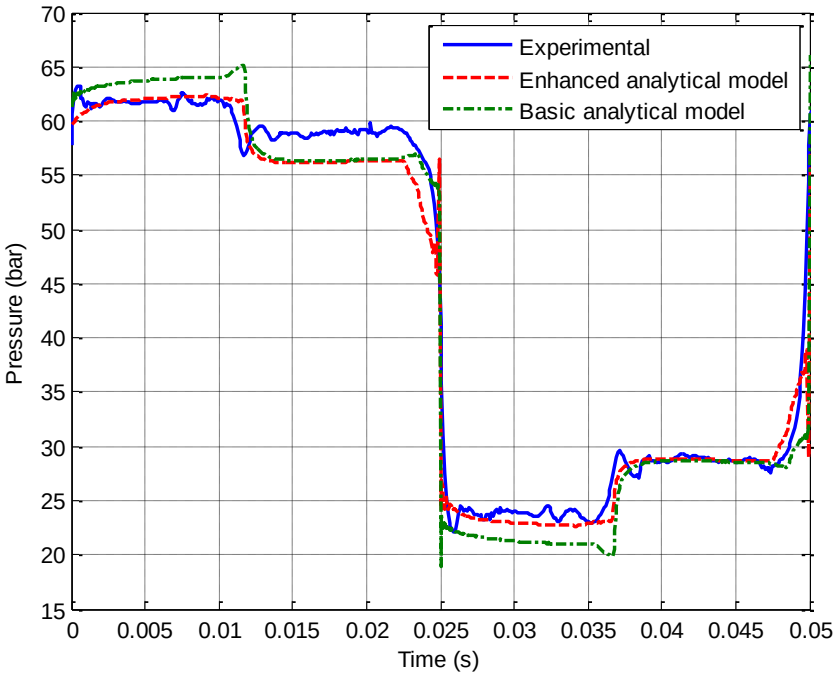

Figure 17 Experimental and analytical upstream inlet pressure of the inertance tube (delivery flowrate = 0L/min; switching frequency = 20Hz; switching ratio = 0.5)

This is a non-optimal switching frequency, and a clear step can be seen at 0.012 s and 0.037 s due to wave propagation effects. The results from the enhanced analytical model and experiments agreed well. Small amplitude differences occurred for the first half cycle, which may be caused by a difference in the resistance of the two ports of the real valve.

With the switching ratio of 0.5, the optimal switching frequency can be calculated from equation (24) to be 40Hz. This condition was modelled and the experimental and analytical upstream inlet pressure of the inertance tube using the basic and enhanced analytical models are shown in Figure 18. The valve switching time is the same as the previous case. The wave propagation effects evident as a disturbance at 0.012s and 0.037s in Figure 17 are not present at the optimal operating conditions.

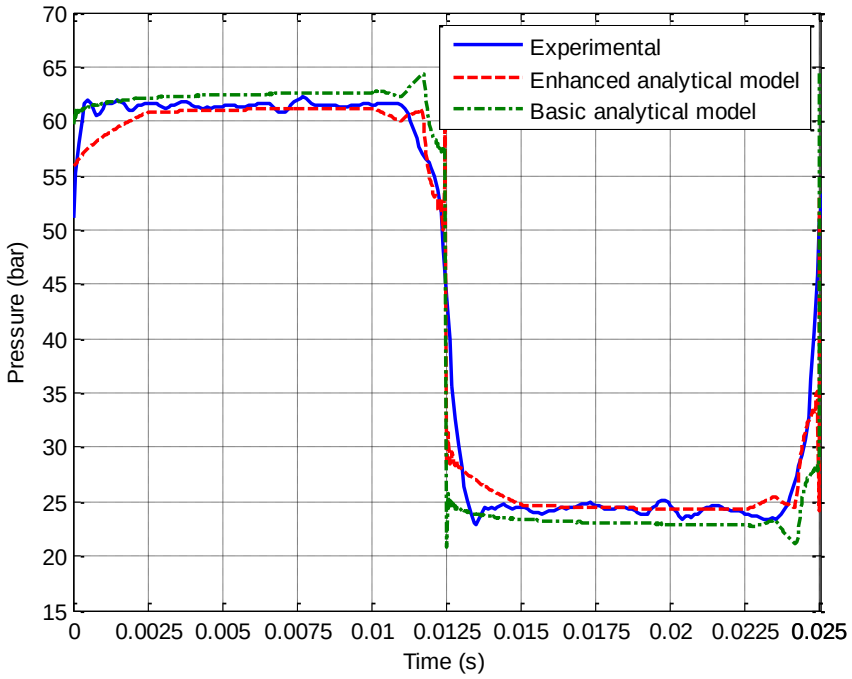

Figure 18 Experimental and analytical upstream inlet pressure of the inertance tube (delivery flowrate = 0L/min; switching frequency = 40Hz; switching ratio = 0.5)

The delivery flowrate was adjusted to 6L/min to investigate the effect of the load flowrate. The same valve, switching transition and leakage resistances were used in the analytical model. Comparisons of the experimental and analytical results are shown in Figures 19 and 20, where good agreements are obtained. Compared with the results predicted from the basic analytical model, the transition dynamics are predicted more accurately by using the enhanced analytical model.

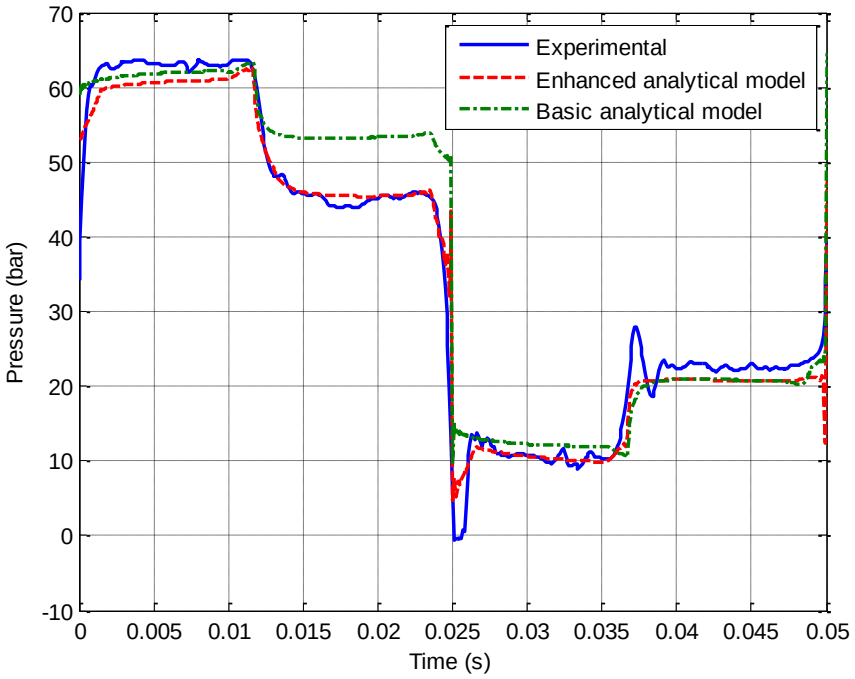

Figure 19 Experimental and analytical upstream pressure of the inertance tube (delivery flowrate = 6L/min; switching frequency = 20Hz; switching ratio = 0.5)

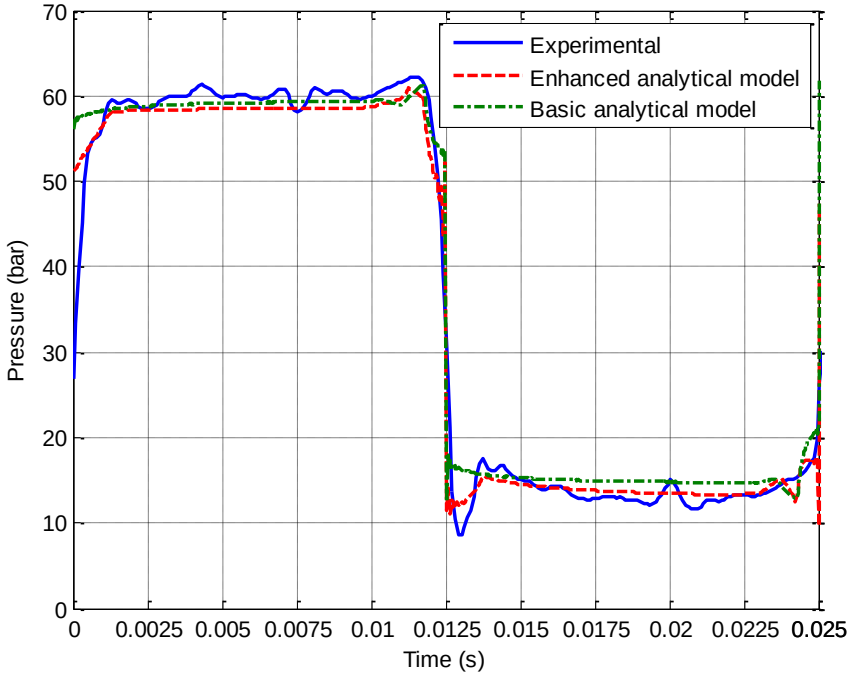

Figure 20 Experimental and analytical upstream pressure of the inertance tube (delivery flowrate = 6L/min; switching frequency = 40Hz; switching ratio = 0.5)

Figure 21 shows the system flow loss by using fixed switching frequencies (20Hz and 40Hz) and varying optimal frequencies, for the switching ratio from 0 to 1. Flowrates of 0L/min and 6L/min were applied respectively. Also shown is the flow loss from the analytical model with optimum switching frequencies. Lower system flow loss occurred when the flow booster operated at the optimal conditions. The analytical and experimental optimal switching curves are approximately symmetrical for zero flowrate (figure 21(a)), but asymmetric with a flowrate of 6L/min (figure 21(b)). The small amplitude difference between the analytical and experimental results in figure 21(b) may be caused by the difference between the estimated and actual leakage area.

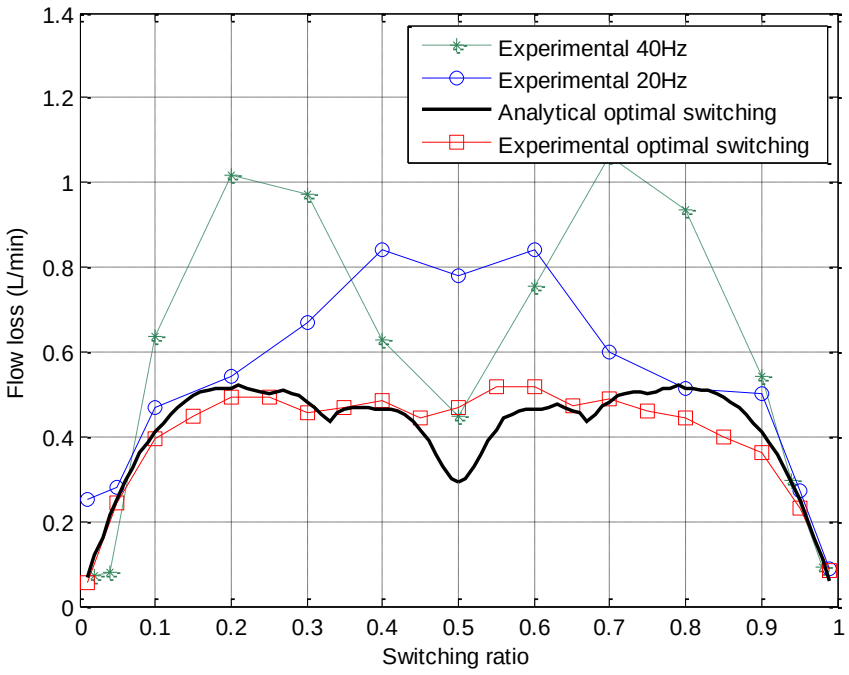

(a) delivery flowrate = 0L/min

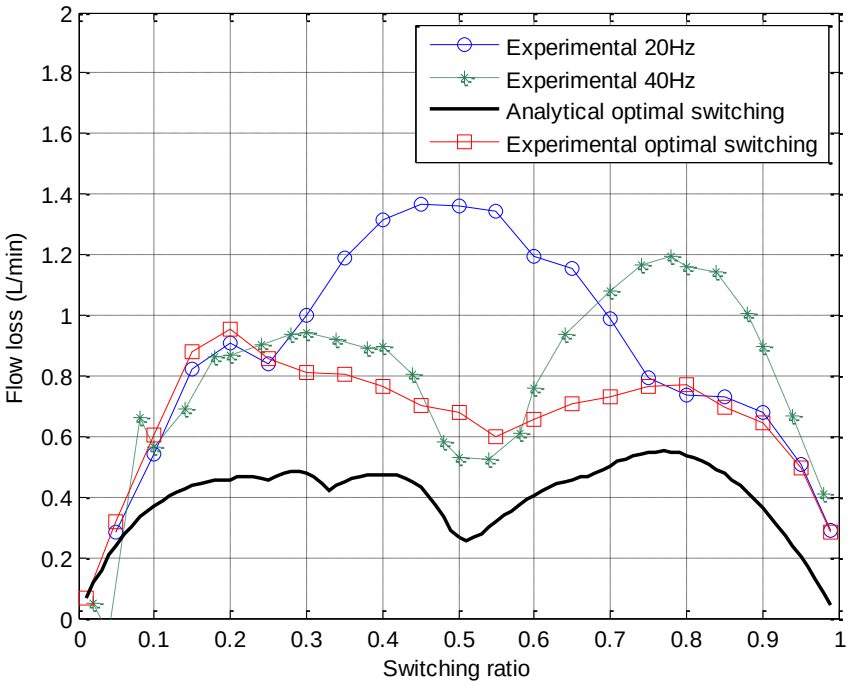

(b) delivery flowrate = 6L/min

Figure 21 System flow loss at the optimal switching conditions

Further experiments were carried out with a switching ratio of 0.5 and a fixed switching frequency of 40Hz. The delivery flowrate was varied from 0L/min to 12L/min.

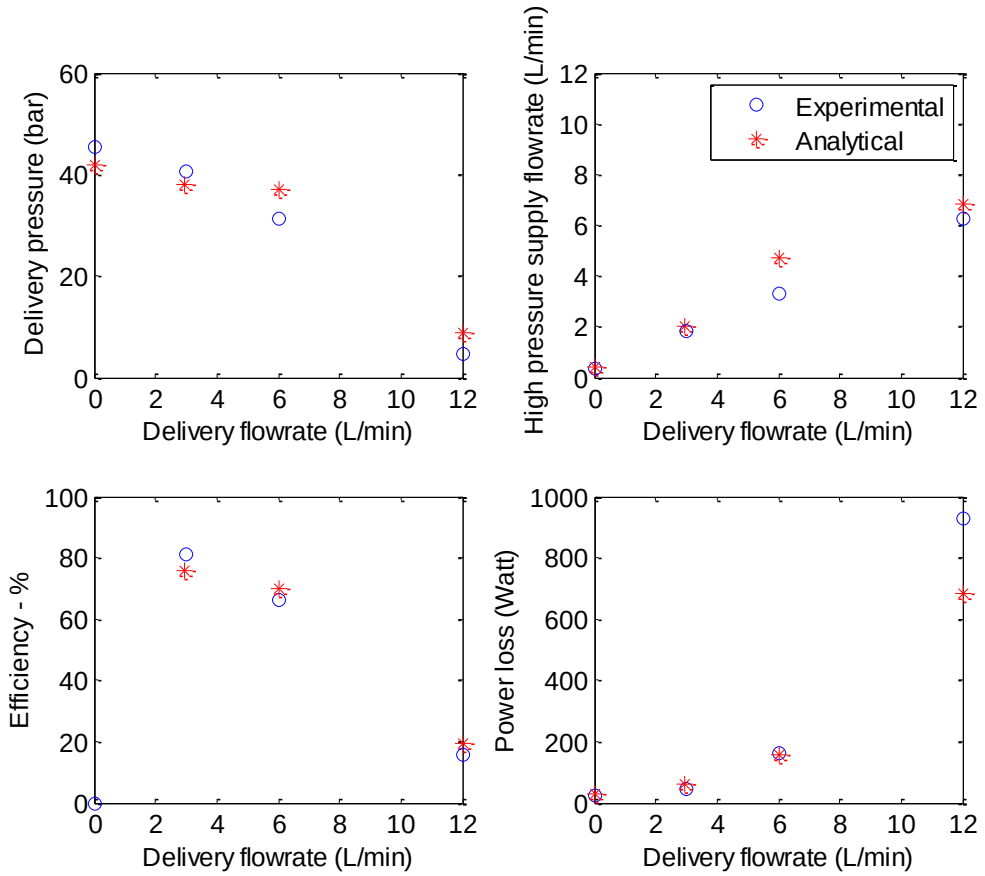

Figure 22 Analytical and experimental results of a flow booster, switching ratio = 0.5, switching frequency = 40 Hz

As shown in Figure 22, more system power loss occurred when delivery flowrate was increased. The SIHS maintained high efficiency (over 70%) with a delivery flowrate of 3L/min and 6L/min. However, efficiency reduces with a larger delivery flowrate. This is because the test rig is actually not an ideal design for very high efficiency. The switching valve and inertance tube used for experiments had high resistances and were not optimized, but they are sufficient for proof of principle of the SIHS and verifying the proposed enhanced analytical model. A more efficient test rig with a low resistance high speed switching valve and a short inertance tube will be studied in future work.

6 Conclusions

The analytical and experimental results show promising performance for the SIHS. The main advantage of the SIHS is that the inherent reactive behaviour of a hydraulic tube is used to control flow and pressure instead of relying on dissipation of power, as in traditional throttling valve-based systems. Using the SIHS, the system efficiency is expected to be increased, whilst the energy cost is decreased.

An enhanced analytical model for investigating the performance of SIHS based on a distributed parameter model in the frequency domain was proposed and has been found to agree well with numerical simulations and experimental results. Compared with the basic analytical models [18], the enhanced model includes the effect of the switching transition dynamics, non-linearity and leakage of the valve. Using the enhanced analytical model, more accurate system dynamics and estimated efficiency can be obtained. It can be treated as a general tool for understanding and analysing the system performance. The enhanced analytical model has been found to be reliable and effective, and is faster to run than the time domain numerical simulations. Moreover, it can be used to optimize the component design and operating conditions of the SIHS due to its high computational speed.

A high-speed switching valve is an important component in a switched hydraulic system. It directly and significantly affects system performance and the selection of the parameters of the tube needs to be done in relation to the valve performance. A high bandwidth valve with a low resistance is desirable. This would increase the system efficiency and decrease energy consumption. Experiments are underway with a high-speed switching valve using a switching frequency over 100Hz [15] and a short

inertance tube of the order of 1m. This will also give the opportunity of using higher delivery flowrate in experiments due to the low resistance of the valve and tube. The enhanced analytical model will be used for this study and will be presented in a later paper. The efficiency will be examined, together with the individual contributions of the loss terms. Also, the pulsation and noise problems will be considered in future work.

Acknowledgements

This work is supported by the UK Engineering and Physical Sciences Research Council under grant number EP/H024190/1, together with Instron, JCB and Parker Hannifin. Their support is greatly appreciated.

References

[1] Johnston, D.N., "A switched inertance device for efficient control of pressure and flow," *Bath/ASME Fluid Power and Motion Control Symposium*, Hollywood, USA, pp.1-8. 2009.

[2] Brown, F.T., "Switched reactance hydraulics: a new way to control fluid power," *Proc. National Conference on Fluid Power, Chicago,* Feb-Mar, pp.25-34, 1987.

[3] Scheidl, R., Manhartsgruber, B and Winkler, B., "Hydraulic switching control – principles and state of the art," *The First Workshop on Digital Fluid Power, Tampere, Finland*, 2008.

[4] Scheidl, R., Manhartsgruber, B., Kogler, H. and Winkler, B.,"The hydraulic buck converter–concept and experimental results," *Proceedings of the Sixth International Conference on Fluid Power*, Dresden, Germany, 2008.

[5] Kogler, H. and Scheidl, R., "Two basic concepts of hydraulic switching converters," *The First Workshop on Digital Fluid Power, Tampere, Finland*, 2008.

[6] Kogler, H., Scheidl, R., Ehrentraut, M., Guglielmino, E., Semini, C. and Caldwell, D.G., "A compact hydraulic switching converter for robotic applications." *In: Proc. Fluid Power and Motion Control, September,* Bath., pp.55-66. 2010.

[7] Scheidl, R., Manhartsgruber, B., Kogler, H. and Winkler, B.,"The hydraulic buck converter–concept and experimental results," *Proceedings of the Sixth International Conference on Fluid Power*, Dresden, Germany, 2008.

[8] Wang, F., Gu,L. and Chen, Y., "A continuously variable hydraulic pressure converter based on high-speed on-off valves," *Mechatronics*, Vol.21, pp.1298-1308, 2011.

[9] Winkler. B., Plockinger. A. and Scheidl. R., "Components for digital and switching hydraulics," *Proc. The First Workshop on Digital Fluid Power, Tampere, Finland*, pp. 53-76, 2008.

[10] Brown, F.T. "A hydraulic rotary switched inertance servo-transformer, " *Journal of Dynamic Systems, Measurement, and Control*, vol. 110, pp.144-150, 1988.

[11] Winkler B., "Development of a fast low-cost switching valve for big flow rates," *3rd PFNI-PhD Symposium on Fluid Power*, Terrassa, Spain, 2004.

[12] Tu, H.C., Rannow, M, Van de Ven, J., Wang, M., Li, P. and Chase, T. "High speed rotary pulse width modulated on/off valve," *Proceedings of the ASME International Mechanical Engineering Congress, Seattle, Washington USA*, pp. 1-14, 2007.

[13] Winkler, B. and Scheidl, R., "Development of a fast seat type switching valve for big flow rates", *The Tenth Scandinavian International Conference on Fluid Power*, Tampere, Finland. 2007.

[14] Van de Ven, J. and Katz, A., "Phase-shift high-speed valve for switch-mode control," *Journal of Dynamic Systems, Measurement, and Control*. Vol.133. 2011.

[15] Kudzma, S., Johnston, D.N., Plummer, A., Sell, N., Hillis, A. and Pan, M., "A high flow fast switching valve for digital hydraulic systems," *The 5th Workshop on Digital Fluid Power, Tampere, Finland*, 2012.

[16] Manhartsgruber, B., Mikota, G. and Scheidl, R., "Modelling of a switching control hydraulic system," *Mathematical and Computer Modelling of Dynamical Systems: Methods, Tools and Applications in Engineering and Related Sciences*. Vol.11, No.3, pp. 329-344, 2005.

[17] Wang, P., Kudzma, S., Johnston, D.N., Plummer, A., Hillis, A.J., "The influence of wave effects on digital switching valve performance," *The Fourth Workshop on Digital Fluid Power*, Linz, Austria, 2011.

[18] De Negri, V.J., Wang, P., Plummer,A. and Johnston, D.N., "Behavioural prediction of step-up switched-inertance hydraulic control systems," *International Journal of Fluid Power* (*Submitted).*

[19] Scheidl, R., Manhartsgruber, B. and Kogler, H., "Mixed time-frequency domain simulation of a hydraulic inductance pipe with a check valve" *Proceedings of the Institution of Mechanical Engineers, Part C: Journal of Mechanical Engineering Science*.vol.225, pp. 2413-2421. 2011.

[20] Pan, M., Johnston, D.N., Plummer, A., Kudzma, S. and Hillis, A., "Theoretical and experimental studies of a switched inertance hydraulic system" *Proceedings of the Institution of Mechanical Engineers, Part I: Journal of Systems and Control Engineering, 2013*

[21] Johnston, D.N., "Measurement and prediction of the fluid borne noise characteristics of hydraulic components and systems." *PhD Thesis, University of Bath.* 1987.

[22] Stecki, J.S and Davis, D., "Fluid transmission lines—distributed parameter models part 1: A review of the state of the art." *Proceedings of the Institution of Mechanical Engineers, Part A: Journal of Power and Energy*. vol. 200, pp.215-228,1986.

[23] Krus, P., Weddfelt, K. and Palmberg, J.O., "Fast pipeline models for simulation of hydraulic system." *Journal of Dynamic Systems, Measurement, and Control*, vol. 116, pp.132-136, 1994.

[24] Johnston, D.N., "The transmission line method for modelling laminar flow of liquid in pipelines." *Proceedings of the Institution of Mechanical Engineers, Part I: Journal of Systems and Control Engineering***,** pp. 1-12.2012.

[25] Johnston, D.N., "An enhanced transmission line method for modelling laminar flow of liquid in pipelines." *Proceedings of the Institution of Mechanical Engineers, Part I: Journal of Systems and Control Engineering*, 2013 (accepted).

Nomenclature

A	Valve opening
A_{leak}	Valve leakage area
B	Bulk modulus
c	Speed of sound
C_d	Discharge coefficient of valve
d	Tube internal diameter
f	Switching frequency
I	Tube inertance
J_0, J_1	Bessel functions of the first kind of orders zero and one
j	Imaginary unit
L	Tube length
n	Number of harmonics
P_n	Fourier coefficient of pressure
P_1'	Fourier coefficient of source pressure p_1
P_2'	Fourier coefficient of source pressure p_2
P_d	Fourier coefficient of delivery pressure
P_i	Fourier coefficient of inlet pressure
p_1	Source pressure of main path
p_2	Source pressure of leakage path
p_d	Delivery pressure
p_1'	Inlet pressure of inertance tube
p_H	High supply pressure
p_L	Low supply pressure
Δp	Pressure drop
Q_d	Fourier coefficient of delivery flowrate
Q_i	Fourier coefficient of inlet flowrate
Q_n	Fourier coefficient of flowrate
q	Flowrate
q_1	Main path flowrate
q_2	Leakage path flowrate
q_i	Inlet flowrate of inertance tube

q_H	Steady state flowrate from the high pressure supply port
$\bar{q}_H$	Average flowrate from the high pressure supply port
q_i	Inlet flowrate of the inertance tube
q_L	Steady state flowrate from the low pressure supply port
$\bar{q}_L$	Average flowrate from the low pressure supply port
q_{loss}	Flow loss
q_m	Average delivery flowrate
R	Overall resistance of the system
R_{non1}	Non-linear characteristics of valve
R_{non2}	Non-linear characteristics of valve
R_t	Resistance of the inertance tube
R_{tr}	Switching transition resistance
R_{up}	Underlap resistance
R_v	Resistance of the high-speed switching valve
T	Switching cycle
t	Time
V_{end}	End volume of inertance tube
V_{up}	Upstream volume of inertance tube
W_{loss}	System power loss
Z_E	Entry impedance
Z'_E	Modified entry impedance
Z_{END}	End impedance
Z_0	Pipe characteristic impedance
α	Switching ratio
λ	Leakage coefficient
ν	Viscosity
ξ	Viscous wave correction factor
ρ	Density
τ	Time constant
ω	Radian frequency